ITU - Telecommunication Standardization Sector Temporary Document CF-061

STUDY GROUP 15 Original: English

Clearwater, Florida, 8 – 12 January 2001

Question: 4/15

SOURCE[1]: IBM

TITLE: G.gen: LDPC coding proposal for G.dmt.bis and G.lite.bis.

ABSTRACT

We present multilevel coding based on binary LDPC codes and investigate transmission performance for ADSL considering the set of requirements formulated in earlier meetings. The obtained results show that advanced coding based on LDPC codes represents a very attractive solution for ADSL systems in terms of performance gains and decoding complexity.

[1] Contact: E. Eleftheriou ele@zurich.ibm.com
S. Ölçer oel@zurich.ibm.com
IBM Zurich Research Laboratory
8803 Rüschlikon, Switzerland

1. Introduction

In the companion contribution [1], we define a family of LDPC codes for ADSL transmission and show the performance that can be achieved by these codes on a binary additive white Gaussian noise (AWGN) channel. In the present contribution, we first define multilevel encoding based on binary LDPC codes. Multilevel encoding is achieved by partitioning the employed symbol set into subsets and applying a Gray-code based symbol mapping. This symbol mapping is different from the one used in traditional trellis-coded modulation. We then address, for the codes of [1], the set of requirements formulated in [2] and [3].

In Section 2, we start by defining multilevel encoding for ADSL using binary LDPC codes. In Section 3, we investigate by simulation the performance of the proposed codes for QAM transmission over a channel affected by AWGN and without or with outer Reed-Solomon coding. In Section 4, we study performance in the presence of impulse noise. We address latency issues in Section 5 and finally give in Section 6 some conclusions.

2. Multilevel LDPC encoding

Transmit symbols are chosen from a 2^b-QAM symbol constellation, where the integer $b = 1$ or $b > 1$ and even. The block diagram of the encoding and symbol mapping functions is shown in Fig. 1.

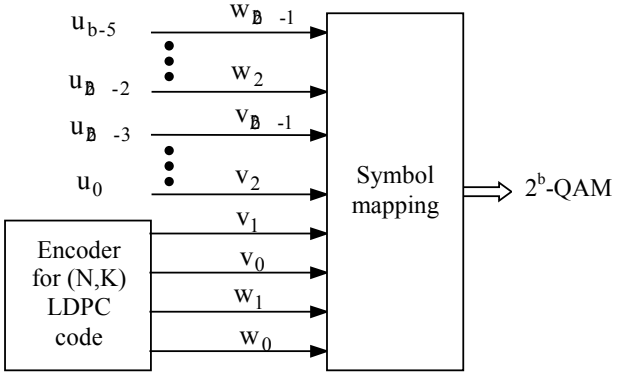

Figure 1: Multilevel LDPC encoding and symbol mapping for 2^b-QAM.

When $b \geq 4$ and even, the two binary b/2-tuples ($v_{b/2-1}$, $v_{b/2-2}$, …, v_1, v_0) and ($w_{b/2-1}$, $w_{b/2-2}$, …, w_1, w_0) independently select two $2^{b/2}$–ary real symbols that represent the real and the imaginary parts, respectively, of the complex QAM symbol to be transmitted. The $2^{b/2}$–ary real symbols belong to the set

A ,

where $L = 2^{b/2}$. Each 2^b-QAM symbol conveys 4 LDPC code bits v_1, v_0, w_1, and w_0 and uncoded bits.

Symbol mapping relies on the partition of the set A into four subsets such that the minimum Euclidean distance between the symbols within each subset is maximized. The 2 least-significant bits (LSBs) (v_1, v_0) [respectively, (w_1, w_0)] label the subsets of A. The remaining b/2-2 most-significant bits (MSBs) ($v_{b/2-1}$, $v_{b/2-2}$, …, v_3, v_2) [respectively, ($w_{b/2-1}$, $w_{b/2-2}$, …, w_3, w_2)] label symbols within a subset. Furthermore, the 2 LSBs and the b/2-2 MSBs separately follow a Gray coding rule.

Note that the described symbol mapping is different from the symbol mapping used in traditional trellis-coded modulation.

When b = 2 [respectively, b = 1], symbol mapping is achieved from the binary 2-tuple (v_0, w_0) [resp., (v_0, 0)], where v_0 and w_0 represent LDPC code bits. A binary value 0 is mapped to +1 and a binary value 1 is mapped to –1. Hence the cases of b = 2 and b = 1 correspond to coded QPSK and BPSK modulations, respectively.

Table 1 gives an example of symbol labeling and mapping for the case of 256-QAM (L = 16). We note that a similar labeling technique has been proposed in [4] for turbo-codes.

L-ary symbol	v_3 (w_3)	v_2 (w_2)	v_1 (w_1)	v_0 (w_0)	Subset number
+15	0	0	0	0	0
+13	0	0	0	1	1
+11	0	0	1	1	2
+9	0	0	1	0	3
+7	0	1	0	0	0
+5	0	1	0	1	1
+3	0	1	1	1	2
+1	0	1	1	0	3
-1	1	1	0	0	0
-3	1	1	0	1	1
-5	1	1	1	1	2
-7	1	1	1	0	3
-9	1	0	0	0	0
-11	1	0	0	1	1
-13	1	0	1	1	2
-15	1	0	1	0	3

Table 1: Example of symbol labeling for the case L = 16.

If coding is achieved with a binary (N,K) LDPC code with K the information block length and N the code length, then multilevel encoding results in a spectral efficiency of

$$\eta = \begin{cases} b + (K - N), & b \geq 4, \text{ bit/s/Hz} \\ bK/N, & b = 1 \text{ or } 2 \end{cases}$$

3. Performance in AWGN

3.1 Performance without outer Reed-Solomon coding

The performance of the LDPC codes specified in Table 1 of [1] was studied by simulation assuming an AWGN channel and 16-QAM, 64-QAM and 4096-QAM. Iterative decoding with the sum-product algorithm was employed, with the number of iterations limited to 20 in order to shorten the simulation time on the computer. As shown in [5], performance can be improved by allowing a larger number of iterations. In all simulations, the number of observed block errors, i.e., codeword errors, was larger than 100.

Figures 2 to 7 show the performance achieved with Code 1 through Code 6 in terms of symbol-error rate (SER) versus the normalized signal-to-noise ratio

,

where E_b/N_0 is the ratio of energy-per-bit to noise-power-spectral-density and η has been previously defined. The corresponding net coding gains, summarized in Table 2, are obtained by extrapolating the simulation results for an SER of 10^{-7} [5]. Note that this can be done since the LDPC codes do not exhibit "error floors" [1].

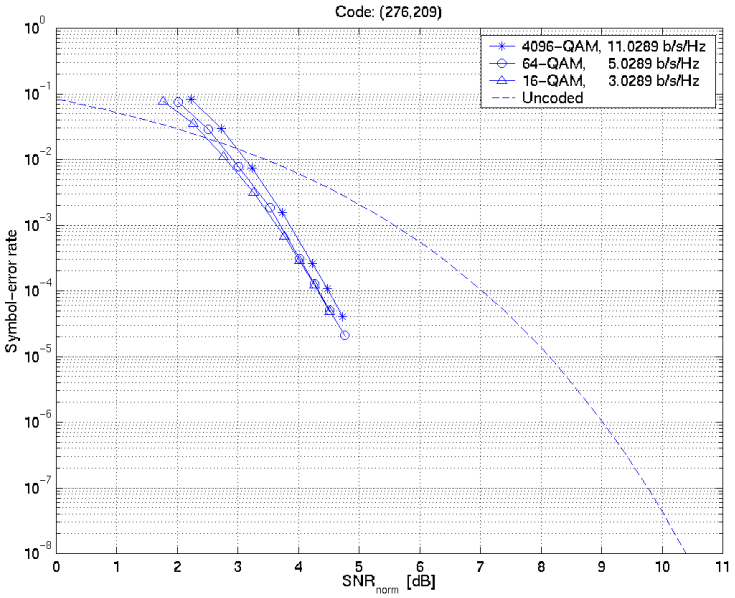

Figure 2: Symbol-error rate versus SNR_{norm} for 16, 64 and 4096-QAM using LDPC Code 1.

Figure 3: Symbol-error rate versus SNR_{norm} for 16, 64 and 4096-QAM using LDPC Code 2.

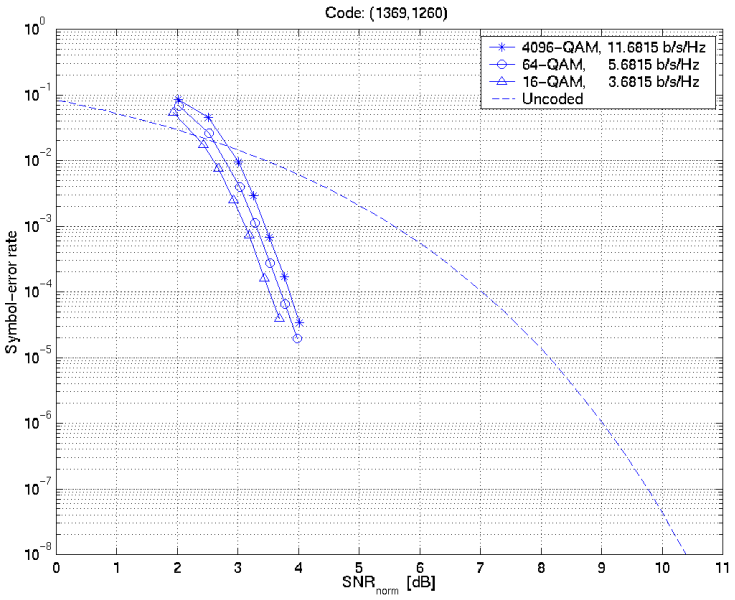

Figure 4: Symbol-error rate versus SNR_{norm} for 16, 64 and 4096-QAM using LDPC Code 3.

Figure 5: Symbol-error rate versus SNR_{norm} for 16, 64 and 4096-QAM using LDPC Code 4.

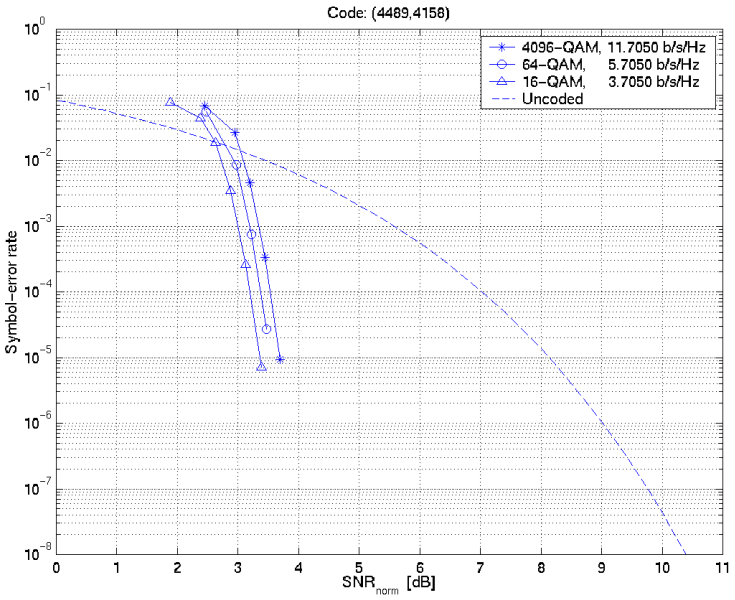

Figure 6: Symbol-error rate versus SNR_{norm} for 16, 64 and 4096-QAM using LDPC Code 5.

Figure 7: Symbol-error rate versus SNR_{norm} for 16, 64 and 4096-QAM using LDPC Code 6.

	16-QAM	64-QAM	4096-QAM
Code 1	3.7 dB (3.03 b/s/Hz)	3.7 dB (5.03 b/s/Hz)	3.5 dB (11.03 b/s/Hz)
Code 2	4.7 dB (3.49 b/s/Hz)	4.5 dB (5.49 b/s/Hz)	4.3 dB (11.49 b/s/Hz)
Code 3	5.4 dB (3.68 b/s/Hz)	5.2 dB (5.68 b/s/Hz)	5.0 dB (11.68 b/s/Hz)
Code 4	6.0 dB (3.66 b/s/Hz)	5.8 dB (5.66 b/s/Hz)	5.6 dB (11.66 b/s/Hz)
Code 5	6.2 dB (3.70 b/s/Hz)	6.0 dB (5.70 b/s/Hz)	5.8 dB (11.70 b/s/Hz)
Code 6	6.4 dB (3.73 b/s/Hz)	6.2 dB (5.73 b/s/Hz)	6.0 dB (11.73 b/s/Hz)

Table 2 : Net coding gains achieved by LDPC codes at a symbol-error rate of 10^{-7} for different QAM constellations. Spectral efficiencies are indicated in parentheses.

3.2 Performance with outer Reed-Solomon coding

For the results presented in this section, we assume an outer Reed-Solomon (RS) code defined in GF(256) having an error correction capability of t = 8 symbols.

We first consider the case when this RS code is concatenated with the inner LDPC Code 4 for 16-QAM transmission. The BER versus E_b/N_0 curves in Fig. 8 show performance at the output of the LDPC decoder and at the output of the RS decoder for the interleaving depths of D = 4 and D = 16. A semi-analytically derived curve is also plotted to indicate performance with infinite interleaving. The figure also shows the BER at the output of the LDPC decoder in the case where no outer RS code is employed. Note that the latter case corresponds to a different spectral efficiency as compared to the previous cases.

Figure 8: Bit-error rate versus E_b/N_0 for a RS and LDPC concatenated coding system, assuming LDPC Code 4 and 16-QAM. Performance at the output of the LDPC decoder (a) and at the output of the RS decoder for D = 4 (b), D = 16 (c), and infinite interleaving (d). Curve (e) shows the BER at the output of the LDPC decoder in the case where no outer RS code is employed.

Figures 9 to 14 show the BER versus E_b/N_0 characteristics for the above RS code concatenated with the LDPC Code 1 through Code 6 and for 16-QAM, 64-QAM, and 4096-QAM. For each case, we show performance for the concatenated system, i.e., performance at the output of the LDPC decoder and performance at the output of the RS decoder for infinite interleaving.

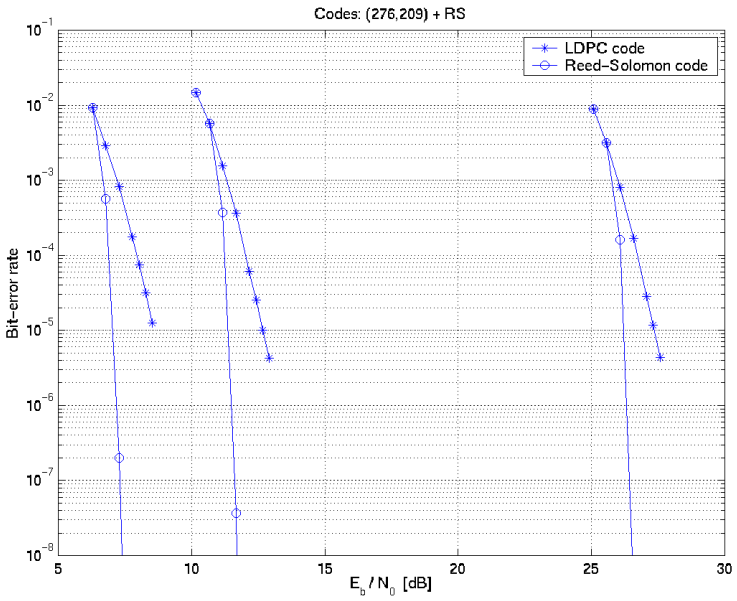

Figure 9: Bit-error rate versus E_b/N_0 for 16, 64 and 4096-QAM (left to right) using outer RS coding and inner LDPC Code 1. Performance at the output of the LDPC decoder and at the output of the RS decoder.

Figure 10: Bit-error rate versus E_b/N_0 for 16, 64 and 4096-QAM (left to right) using outer RS coding and inner LDPC Code 2. Performance at the output of the LDPC decoder and at the output of the RS decoder.

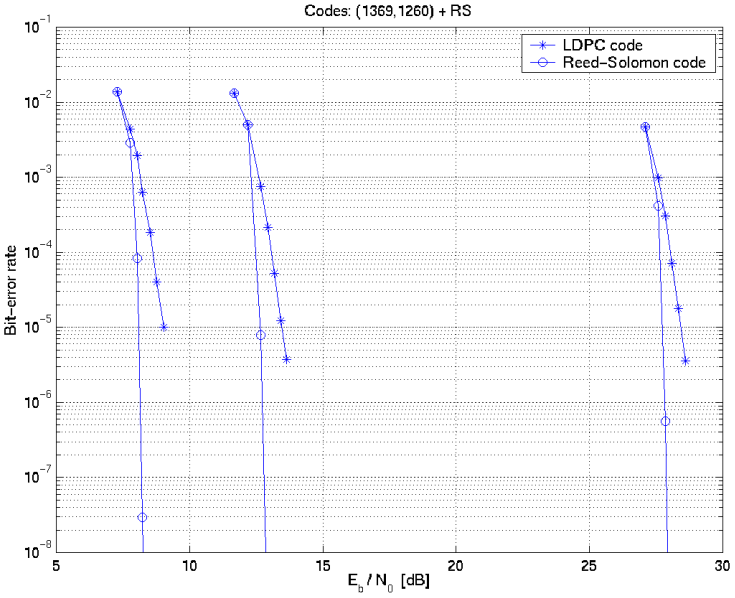

Figure 11: Bit-error rate versus E_b/N_0 for 16, 64 and 4096-QAM (left to right) using outer RS coding and inner LDPC Code 3. Performance at the output of the LDPC decoder and at the output of the RS decoder.

Figure 12: Bit-error rate versus E_b/N_0 for 16, 64 and 4096-QAM (left to right) using outer RS coding and inner LDPC Code 4. Performance at the output of the LDPC decoder and at the output of the RS decoder.

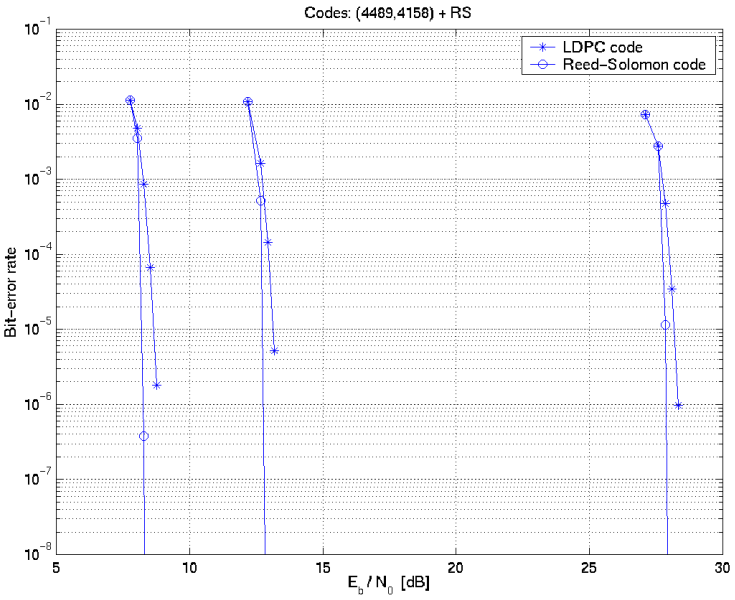

Figure 13: Bit-error rate versus E_b/N_0 for 16, 64 and 4096-QAM (left to right) using outer RS coding and inner LDPC Code 5. Performance at the output of the LDPC decoder and at the output of the RS decoder.

Figure 14: Bit-error rate versus E_b/N_0 for 16, 64 and 4096-QAM (left to right) using outer RS coding and inner LDPC Code 6. Performance at the output of the LDPC decoder and at the output of the RS decoder.

The coding gains achieved by the outer RS code with infinite interleaving obtained from these figures are summarized in Table 3 for a BER of 10^{-7}.

Outer code	Inner LDPC code	16-QAM	64-QAM	4096-QAM
(255,239) RS code	Code 1	2.4 dB	2.1 dB	2.0 dB
	Code 2	2.0 dB	1.8 dB	1.6 dB
	Code 3	1.5 dB	1.3 dB	1.2 dB
	Code 4	1.0 dB	0.86 dB	0.81 dB
	Code 5	0.61 dB	0.60 dB	0.57 dB
	Code 6	0.52 dB	0.48 dB	0.41 dB

Table 3: Coding gains due to RS coding at a bit-error rate of 10^{-7} assuming infinite interleaving. The values indicated do not include the coding gain due to the inner LDPC code (see Table 2).

4. Performance in the presence of impulse noise

To determine performance in the presence of burst or impulse noise, we follow the procedure described in [2]. The impulse noise level is defined in dB with respect to the reference noise level corresponding to a signal-to-noise ratio of 21.5 dB and 45.5 dB for the two cases of 4 bits per tone and 12 bits per tone, respectively. The results of the simulations are summarized in Table 4, where we give the average number of bit errors per impulse-noise event without outer RS coding and with outer RS coding using the GF (256) RS code with an error correcting capability of t = 8 and an interleaving depth of D = 16.

Bit/tone	Tones	Code #	+2.5dB	+5dB	+7.5dB	+10dB	+12.5dB	+15dB
4	100	1	0 (0)	0 (0)	0 (0)	15 (0)	67 (0)	109 (0)
		2	0 (0)	0 (0)	0 (0)	28 (0)	73 (0)	119 (0)
		3	0 (0)	0 (0)	0 (0)	31 (0)	77 (0)	123 (0)
		4	0 (0)	0 (0)	0 (0)	26 (0)	90 (2)	132 (3)
		5	0 (0)	0 (0)	0 (0)	11 (0)	75 (0)	91 (0)
		6	0 (0)	0 (0)	0 (0)	0 (0)	73 (0)	117 (0)
	200	1	0 (0)	0 (0)	0 (0)	21 (0)	127 (38)	216 (186)
		2	0 (0)	0 (0)	0 (0)	36 (0)	83 (23)	135 (112)
		3	0 (0)	0 (0)	0 (0)	57 (0)	144 (33)	239 (183)
		4	0 (0)	0 (0)	0 (0)	55 (0)	150 (58)	242 (213)
		5	0 (0)	0 (0)	0 (0)	54 (2)	152 (57)	251 (207)
		6	0 (0)	0 (0)	0 (0)	28 (0)	132 (29)	243 (195)
12	100	1	0 (0)	0 (0)	0 (0)	35 (0)	97 (11)	151 (61)
		2	0 (0)	0 (0)	3 (0)	52 (0)	108 (7)	168 (53)
		3	0 (0)	0 (0)	1 (0)	56 (0)	112 (2)	176 (51)
		4	0 (0)	0 (0)	0 (0)	49 (1)	106 (2)	165 (30)
		5	0 (0)	0 (0)	0 (0)	46 (0)	108 (13)	168 (45)
		6	0 (0)	0 (0)	0 (0)	18 (0)	107 (3)	167 (25)
	200	1	0 (0)	0 (0)	0 (0)	64 (11)	193 (174)	309 (308)
		2	0 (0)	0 (0)	5 (0)	101 (22)	206 (184)	326 (326)
		3	0 (0)	0 (0)	7 (0)	97 (12)	216 (187)	343 (320)
		4	0 (0)	0 (0)	0 (0)	94 (8)	216 (167)	340 (310)
		5	0 (0)	0 (0)	0 (0)	89 (7)	212 (168)	337 (315)
		6	0 (0)	0 (0)	0 (0)	70 (5)	215 (120)	331 (244)

Table 4 : Average number of bit errors per impulse-noise event with and without outer RS coding (latter case indicated in parentheses). The impulse-noise level is incremented in steps of +2.5 dB. An impulse-noise level of 0 dB corresponds to signal-to-noise ratio values of 21.5 dB and 45.5 dB for the two cases of 4 bits/tone and 12 bits/tone, respectively.

Table 4 shows that LDPC codes are as robust as turbo codes in the presence of burst noise [4], [6]. Note that turbo codes owe this robustness to the use of interleavers whereas no interleavers are employed for the LDPC codes.

5. Latency

In [2], latency is defined as the total latency of encoding and decoding. Accordingly, we will take total latency as being (approximately) equal to twice the latency needed for encoding. Table 5 gives latencies associated with the various LDPC codes for the cases of 4 or 12 bits/tone and a total number of 100 and 200 tones.

Bit/tone	Tones	LDPC Code	Encoding latency in DMT-symbol time	Total latency in ms
4 or 12	100	Code 1	--	--
		Code 2	1	0.50
		Code 3	3	1.50
		Code 4	5	2.50
		Code 5	11	5.50
		Code 6	19	9.50
	200	Code 1	--	--
		Code 2	--	--
		Code 3	1	0.50
		Code 4	2	1.00
		Code 5	5	2.50
		Code 6	9	4.50

Table 5: Latency associated with the different LDPC codes.

Clearly, the set of LDPC codes that has been defined in Section 2 allows encoding to be contained to within 1 DMT-symbol time for any valid number of information bits per DMT symbol. The corresponding coding gains depend on the actual number of information bits to be conveyed by a DMT symbol and the specific code parameters and spectral efficiency.

6. Summary and conclusion

We have presented a family of LDPC codes and the specific symbol mapping function to be used for ADSL transmission. Performance under AWGN and impulse noise has been determined by simulation, also including outer Reed-Solomon coding. Latency associated with the proposed codes has been determined.

We therefore recommend to use LDPC codes as described in this contribution and in [1] for advanced coding in G.dmt.bis and G.lite.bis.

References

[1] "LDPC codes for G.dmt.bis and G.lite.bis," Temporary Document CF-060, Study Group 15/4, Clearwater, FL, 8-12 Jan. 2001.

[2] "Coding ad hoc report," Temporary Document BA-108, Study Group 15/4, Antwerp, Belgium, 19–23 June 2000.

[3] "Report of the ad hoc on improved coding gain," Temporary Document BI-110, Study Group 15/4, Goa, India, 23–27 October 2000.

[4] "A turbo TCM scheme with low decoding complexity," Temporary Document BI-090, Study Group 15/4, Goa, India, 23–27 October 2000.

[5] "Low-density parity-check codes for DSL transmission," Temporary Document BI-095, Study Group 15/4, Goa, India, 23-27 Oct. 2000.

[6] "Results of the requirements requested in the coding ad hoc report (BA-108R1) for the proposed turbo codes for ADSL modems by VoCAL Technologies Ltd in BA-020R1," Temporary Document HC-073, Study Group 15/4, Huntsville, Canada, 31 Jul. – 4 Aug. 2000.